

Control Strategy of Aileron's Force-fight

Ying Zhang and Zhaohui Yuan

School of automation, Northwestern Polytechnical University
Zhangying_1102@163.com

Abstract

Due to adopting redundant actuation system, force-fight phenomenon appears on aileron's plane, which would accelerate the fatigue of rudder surface material and loss power. Effective measures must be taken to reduce or eliminate this phenomenon. On the basis of analyzing the control structure of aileron, precisely modeling the control system, and taking system's nonlinear links into account. The correctness of the model is verified by experiment. Then control strategy of reducing the fighting-force is considered from two aspects of both static and dynamic. The method of using the force equilibrium with pure integral part is to use the integral of each channel's pressure differential to compensate the displacement control signal; The simulation results show that this method can basically eliminate static fighting-force. In order to reduce the fighting-force during dynamic process at the same time, adopting the PID controller for force equilibrium on the basis of static policy. This method can realize the displacement compensation during the dynamic process. The simulation results show that, after adopting the PID control strategy, the static fighting-force can be eliminated basically, and the dynamic fighting-force can be reduced by about 80%.

Keywords: *force-fight, nonlinear model, force equilibrium, control strategy*

1. Introduction

Cross linking and interference problem between channels of redundant steering gears (that is multiple single steering gear driving a comprehensive shaft) which are used on aircraft and space vehicles is called force-fight phenomenon [1, 2]. Redundant steering gear is the key component of the flight control system. In order to improve system's reliability and security usually adopt 2 or 3 actuators to control the rudder surface simultaneously. The discrepancy of pipe's length, the error accumulation caused by manufacture and installation and long time working wear of actuators and servo-valves will both lead to the difference of the output displacement between actuators which will accelerate the fatigue of rudder surface material, reduce the service life, and increase the loss of energy, so it is necessary to balance the actual force between channels to ensure the fighting-force is affordable and reduce the adverse impacts on the control surface[3-5]. Boeing-777 adopts the differential pressure sensors to transmit fighting-force signal to the instruction level to equilibrate the force to reduce fighting-force [6]. In F/A-18 the two channels share a master control valve, this kind of design can ensure the synchronization of the two actuators by controlling the precision of the valve core [7]. In Su30 a throttle valve is used to connect the two cavities to reduce fighting-force [8]. This paper studies the fly-by-wire control system of aileron plane which adopts the SHA method to control actuators, On the basis of analyzing the control structure of aileron, precisely modeling the control system, the fixed stiffness of actuator and connective stiffness between rod and rudder surface are taken into account in this model, and the pressure loss of all pipes is also considered [9-13]. The test results show that this model can reflect the working process of actual system precisely. In order to reduce fighting-force, the control strategy is considered from two aspects of static and dynamic respectively. The static force-fight strategy adopts the integral of the force as channels' displacement compensation signals

[14, 15]. This method is proved to be effective in eliminating static fighting-force. To reduce the dynamic fighting-force, using PID controller instead of pure integral part to adjust the dynamic performance, this method can effectively reduce the fighting-force during dynamic process.

2. Structure Diagram and Working Principle

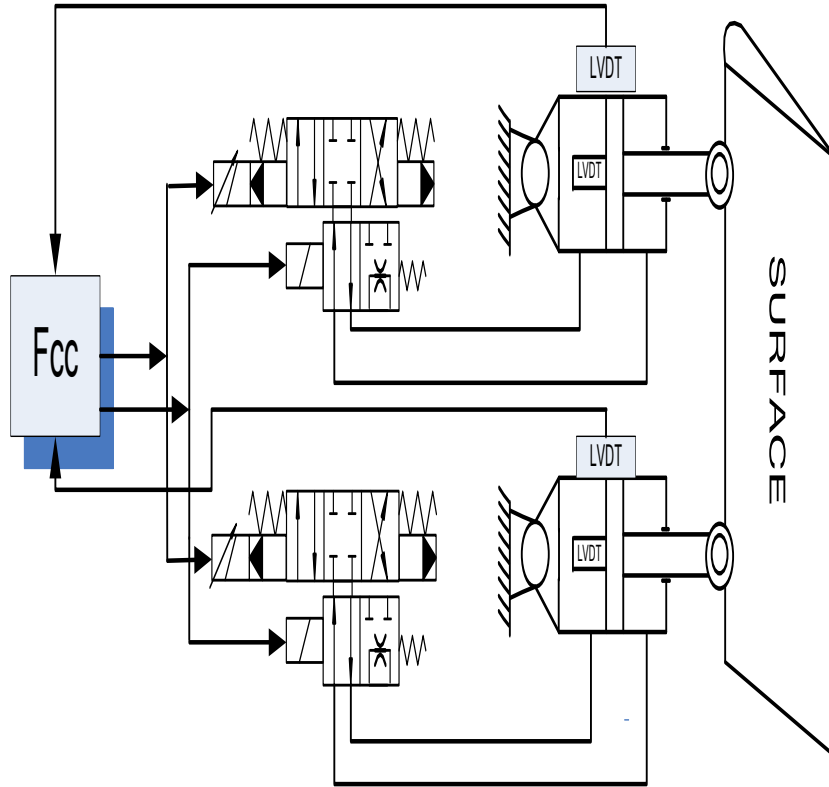


Figure 1. Structure Diagram

In Figure 1, the rudder control system is a dual channel SHA system. The input voltage signal is converted to corresponding current signal in FCC to control the output flow rate of the servo-valve and thereby pressure differential is produced between two cavities to drive the rudder surface. The two actuators has feedback channel respectively. The piston's displacement signal is transmitted to the input terminal through sensor and compared with the given voltage signal to obtain a new voltage signal to adjust the flow rate of servo-valve to ensure rudder surface's rotation angle is basically the same as the expectation. The fighting-force is defined as the difference of the output force the two actuators.

3. Mathematical Model

3.1. Flow Equation of Servo-valve

The dynamic characteristic of electro-hydraulic servo-valve is usually expressed in transfer function during the analysis and design of electro-hydraulic servo system. From the practical perspective, the complex function can be generally simplified to a second order oscillation link. In this paper the function of the servo-valve is presented as:

$$G_{sv}(s) = \frac{x_v(s)}{i(s)} = \frac{K_{sv}}{\frac{s^2}{\omega_{sv}^2} + \frac{2\zeta_{sv}}{\omega_{sv}}s + 1} \quad (1)$$

Where x_v is the displacement of valve core; i is the input current; ω_{sv} is the natural frequency of the servo-valve; ζ_{sv} is the damping ratio; k_{sv} is the displacement gain.

The parameters of the servo-valve are as follows: the rated supply oil is $21MPa$, the rated current is $\pm 10mA$, the rated flow rate is $60L/min$, the natural frequency is $200rad/s$, the damping ratio is 0.7 , the maximal displacement of valve core is $0.57mm$, and the displacement gain is 0.057 .

The flow equation of servo-valve can be obtained in equation (2) according to the above analysis:

$$\left\{ \begin{aligned} Q_1 &= c_v w x_v \sqrt{\frac{2}{\rho}(p_s - p_1)} = c_v w \frac{i \times K_{sv}}{\frac{s^2}{\omega_{sv}^2} + \frac{2\zeta_{sv}}{\omega_{sv}}s + 1} \sqrt{\frac{2}{\rho}(p_s - p_1)} \\ Q_2 &= c_v w x_v \sqrt{\frac{2}{\rho}p_2} = c_v w \frac{i \times K_{sv}}{\frac{s^2}{\omega_{sv}^2} + \frac{2\zeta_{sv}}{\omega_{sv}}s + 1} \sqrt{\frac{2}{\rho}p_2} \end{aligned} \right. \quad (2)$$

Where Q_1, Q_2 is the input and output flow rates of servo-valve respectively, w is the gradient area of servo-valve.

3.2. Continuity Equation of Actuator

The asymmetric actuator is adopted for one cavity has a piston rod and another one has not so the effective area of the two cavities is not the same, the actuator work in two ways as show in Figure 2.

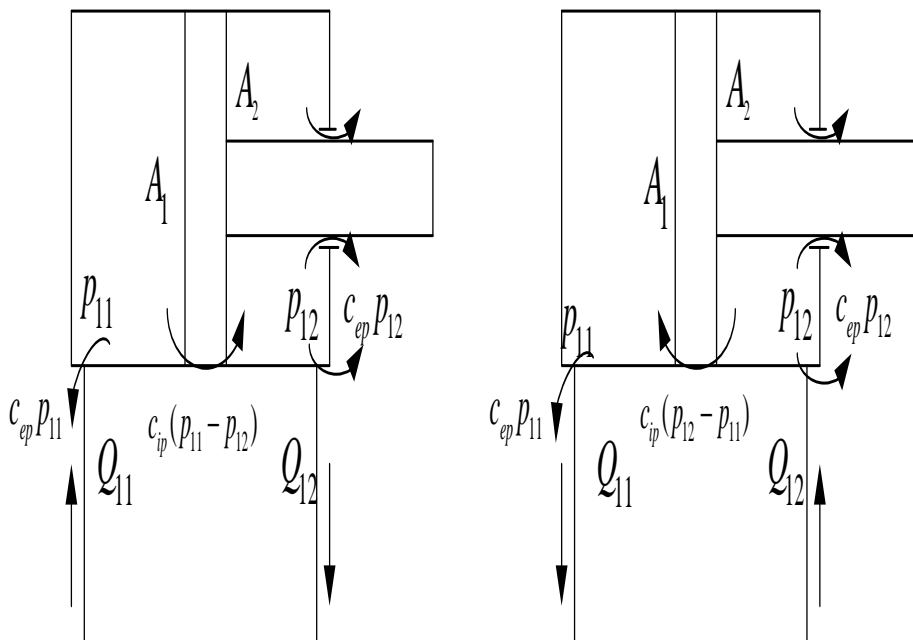


Figure 2. Working Diagram of the Actuator

The continuity equation of actuator is presented as:

$$\begin{cases} Q_{11} = A_1 \frac{dx_{r1}}{dt} + \frac{(x_{01} + x_{r1})A_1}{E_y} \frac{dp_{11}}{dt} + C_{ip}(p_{11} - p_{12}) + C_{ep}(p_{11} - p_0) \\ Q_{12} = A_2 \frac{dx_{r1}}{dt} - \frac{(x_{02} - x_{r1})A_2}{E_y} \frac{dp_{12}}{dt} + C_{ip}(p_{11} - p_{12}) - C_{ep}(p_{12} - p_0) \end{cases} \quad (3)$$

Where p_{11} the pressure of left cavity, p_{12} is the pressure of right cavity, Q_{11} is the flow rate which flow into the left cavity, Q_{12} is the flow rate which flow out from the right cavity. A_1 is the effective area of head port, A_2 is the effective area of rod port. x_{01} is the initial displacement of head port, x_{02} is the initial displacement of rod port, C_{ip} and C_{ep} are the internal and external leakage coefficient respectively, E_y is the modulus of volume elasticity. x_{r1} is the displacement of the rod.

In the course of work the head port is hinged-supported, cause the fixed stiffness between the fixed point to cylinder is considered, the connection part may have certain deformation during the dynamic process which means that the cylinder body itself has certain displacement and it is set to x_c , so the rod's displacement relative to the cylinder is set to $(x_r - x_c)$, so the continuity equation is expressed as:

$$\begin{cases} Q_{11} = A_1 \frac{dx_{r1} - x_{c1}}{dt} + \frac{(x_{01} + x_{r1} - x_{c1})A_1}{E_y} \frac{dp_{11}}{dt} + C_{ip}(p_{11} - p_{12}) + C_{ep}(p_{11} - p_0) \\ Q_{12} = A_2 \frac{dx_{r1} - x_{c1}}{dt} - \frac{(x_{02} - (x_{r1} - x_{c1}))A_2}{E_y} \frac{dp_{12}}{dt} + C_{ip}(p_{11} - p_{12}) - C_{ep}(p_{12} - p_0) \end{cases} \quad (4)$$

3.3. Dynamic Equilibrium Equation

3.3.1. Equilibrium Equation of Piston Rod: The output force of piston rod that is the pressure differential of the two cavities should be balanced with the load force, which including the inertia force of rod and load, viscous damping force, friction and elastic load force which is caused by the deformation of the piston rod. The dynamic equilibrium equation of piston rod is presented as:

$$\begin{cases} p_{11}A_1 - p_{12}A_2 = m_r \frac{d^2 x_{r1}}{dt^2} + B_r \frac{d(x_{r1} - x_{c1})}{dt} + f_{s1} + f_L \\ f_{s1} = (x_{r1} - x_s)K_{s2} \end{cases} \quad (5)$$

Where: m_r is the equivalent mass of both piston and load, B_r is the viscous damping coefficient of piston and load, K_{s2} is the joint stiffness between piston rod and load, f_L is the frictional resistance of piston rod.

3.3.2. Equilibrium Equation of Cylinder: The force applied to the actuator cylinder include the hydraulic pressure of the two cavities, the inertia force of the cylinder, viscous damping force and the force caused by the deformation of the hinged-supported part. The equilibrium equation of cylinder can be expressed as:

$$p_{11}A_1 - p_{12}A_2 = -m_c \frac{d^2 x_{c1}}{dt^2} - B_r \frac{d(x_{c1} - x_{r1})}{dt} - K_{s1}x_{c1} \quad (6)$$

Where: m_c is the mass of cylinder, K_{s1} is the stiffness where the cylinder is hinged-supported.

3.3.3. Equilibrium Equation of Rudder Surface: The system has two inputs, servo-valve's current input and the air load torque T_a , the output is the rotation angle of the rudder surface θ , the control surface is in rotation motion and the rod is in linear motion, in order to simplify the calculation, the rotation angle can be equivalent to displacement x_s , and the air load torque can be equivalent to load force F_L , and under the precondition of the push and pull displacement of the piston rod is very small, x_s and F_L are proportional to θ and T_a respectively. The equivalent mass of the rudder surface is proportional to its moment of inertia J which can be expressed as:

$$m_s = k^2 J \quad (7)$$

Where: k is defined as the ratio of maximum rotation angle of the rudder surface θ_{\max} and the maximum working stroke of the actuator $x_{t\max}$ which is presented as:

$$k = \theta_{\max} / x_{t\max} \quad (8)$$

So the equilibrium equation of rudder surface is presented as:

$$f_{s1} + f_{s2} - F_L = m_s \ddot{x}_s \quad (9)$$

Where: $f_{s1} = (x_{t2} - x_s)K_{s2}$

3.4. Frictional Pressure Loss of Pipeline

Considering the pressure loss of the pipeline from servo-valve to cylinder, the relationship of the pressure in the two cavities and the pressure of the servo-valve's import and export can be expressed as:

$$\begin{cases} p_{11} = p_1 - \Delta p_{11} \\ p_{12} = p_2 + \Delta p_{12} \end{cases} \quad (10)$$

Where: Δp_{11} is the pressure loss on the way the hydraulic oil flow into the actuator cylinder from servo-valve, Δp_{12} is the pressure loss on the way the hydraulic oil flow back to servo-valve from the cylinder.

The frictional pressure loss not only include the pressure loss when oil pass through the straight pipeline but also include the pressure loss when oil pass through the bended place of pipeline, the two condition have different formulations.

The formulation of the pressure loss of straight pipeline is presented as:

$$\Delta p_\lambda = \lambda \frac{l}{d} \frac{\rho v^2}{2} \quad (11)$$

Where: Δp_λ is the frictional pressure loss, λ is the frictional resistance factor, l is the length of the pipeline, d is the diameter of the pipeline, v is the average velocity of flow in pipeline

This formulation can be not only applied to laminar flow but also applied to turbulent flow, but the value of the resistance factor λ is different, In the process of calculation the Renault coefficient is real-time monitored to confirm the value of resistance factor λ which can be expressed as:

$$\begin{cases} \lambda = 75/Re & (Re < 2320) \\ \lambda = 0.3164/Re^{0.25} & (Re > 2320) \end{cases} \quad (12)$$

When the pipeline is bended the frictional pressure loss should be considered, for circular tube the pressure loss of the bended place in pipeline is presented as:

$$\Delta p_{\xi} = \xi \frac{\rho v^2}{2} = \frac{7.878 \rho}{\pi^2 d^4} Q^2 \quad (13)$$

Where: Δp_{ξ} is called local pressure loss, ξ is the local resistance factor, Q is the flow rate when the oil flow through the bended places of pipeline.

4. Experimental Verification

The main simulation parameters are shown in Table 1

Table 1. Main Simulation Parameters

Oil pressure	Return pressure	Fixed stiffness	Joint stiffness	Internal leakage coefficient
21MPa	0MPa	1e8N/m	1e8N/m	1.6e-13
External leakage coefficient	Piston quality	Actuator quality	Oil density	Piston diameter
1e-18	2kg	12kg	850kg/m ³	0.1m

The input voltage signal used in the experiment is a sine signal, its amplitude is 0.5V, and the frequency is from 1Hz to 10Hz. The dead zone of servo-valve 1 is 0.012mm and the dead zone of servo-valve 2 is 0.024mm and the system is no-load. The results of experiment and simulation are show in Tab 2.

Table 2. Contrast of the Results of Experiment and Simulation

Frequency/Hz	1	2	3	4	5
Simulation FF/KN	3.88	2.38	2	1.73	1.52
Actual FF/KN	4.09	2.52	2.23	1.81	1.68
Frequency/Hz	6	7	8	9	10
Simulation FF/KN	1.36	1.23	1	0.74	0.51
Actual FF/KN	1.54	1.44	1.26	0.79	0.62

As show in Table 2 the simulation results is very close to the actual but is always less than the actual, this is due to the ignorance of the difference of the mechanical transmission parts' clearance. In general the mathematical model can well simulate the actual and provides an accurate simulation platform for subsequent analysis.

5. Research of Control Strategy

5.1. Elimination of Static Force-fight

The static force-fight is caused by the inconsistency of redundant actuator. The servo-valve's dead zone, working clearance of mechanical parts and the difference of the pipelines' length and inevitable wear during the production process will all lead to the position error of the two actuators, this error can explained as to be produced by the closed loop stiffness of the actuator system and the joint stiffness from the actuator to rudder surface.

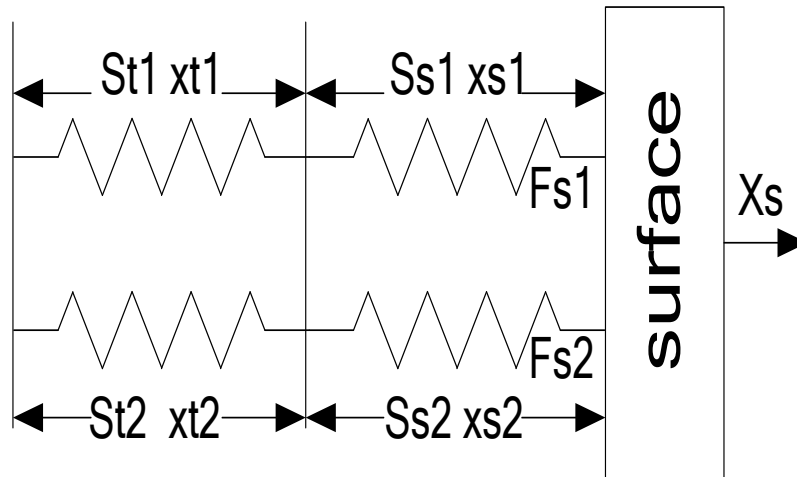


Figure 3. System Static Performance

Where: St is the closed loop of actuator system, Ss is the joint stiffness from actuator to rudder surface.

The displacement of rudder surface is equal to the displacement of each channel which can be expressed as:

$$x_s = x_{t1} + x_{s1} = x_{t2} + x_{s2} \quad (14)$$

Where: x_t is the displacement of piston and x_s is the elastic deformation of piston rod.

The expected elongation of the piston rod is set to x_r , so the displacement of piston and the deformation of piston rod in static can be calculated as:

$$\begin{cases} x_r - x_{t1} = s_{t1}^{-1} \times F_{s1} \\ x_r - x_{t2} = s_{t2}^{-1} \times F_{s2} \\ x_{s1} = -s_{s1}^{-1} F_{s1} \\ x_{s2} = -s_{s2}^{-1} F_{s2} \end{cases} \quad (15)$$

Substituting equation (14) to equation (15), leading to:

$$\begin{cases} s_{t1}^{-1} F_{s1} + s_{s1}^{-1} F_{s1} = s_{t2}^{-1} F_{s2} + s_{s2}^{-1} F_{s2} \\ F_{s1} + F_{s2} = F_L \end{cases} \quad (16)$$

In order to reduce or eliminate the static force-fight the effective method is to make F_{s1} and F_{s2} to be equaled as much as possible. In the equation (16) St and Ss can be changed to achieve this purpose, but the main parameters of the system have been confirmed and it is not easy and unrealistic to change the parameters. A simple and effective method of adding displacement offset E_0 in the equation (16) is feasible which can be realized by adjusting the displacement signals obtained by sensors and finally make $F_{s1} = F_{s2}$:

$$\begin{cases} s_{t1}^{-1} f_{s1} + s_{s1}^{-1} F_{s1} = s_{t2}^{-1} F_{s2} + s_{s2}^{-1} F_{s2} + E_0 \\ F_{s1} = F_{s2} = \frac{1}{2} F_L \end{cases} \quad (17)$$

According to the analysis above, the value of fighting-force can be used as the displacement compensation signal by a series of transformation. If the output force is greater in channel 1 the algorithm will make the displacement compensation E_{01} smaller and vice versa. So the control current can be adjusted according to the analysis above and finally make the output force to be equaled. The control block diagram is presented in Figure 4.

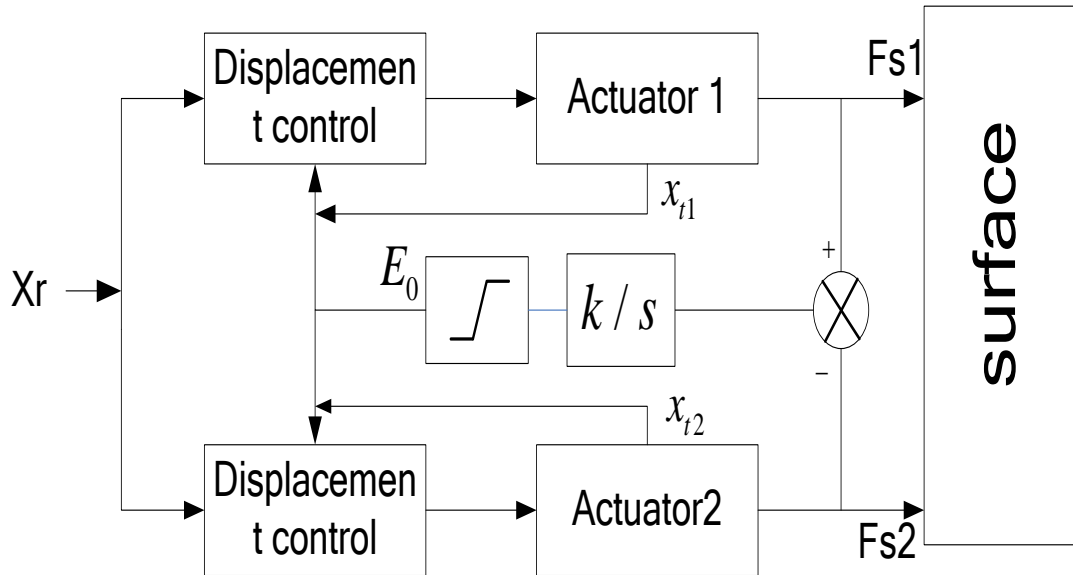


Figure 4. Control Diagram of Static Force-fight

In practical, due to the measurement of the pressure differential of the two cavities is more efficient and low cost, and according to equation (5) the force loss is actually very small which can be expressed as:

$$f_s \approx P_L A \quad (18)$$

Where: P_L is the load pressure differential.

So it is reasonable to adopt the load pressure differential as the displacement compensation signal of each channel. The block diagram of using the integral of load pressure differential to compensate position signal is represented in Figure 5

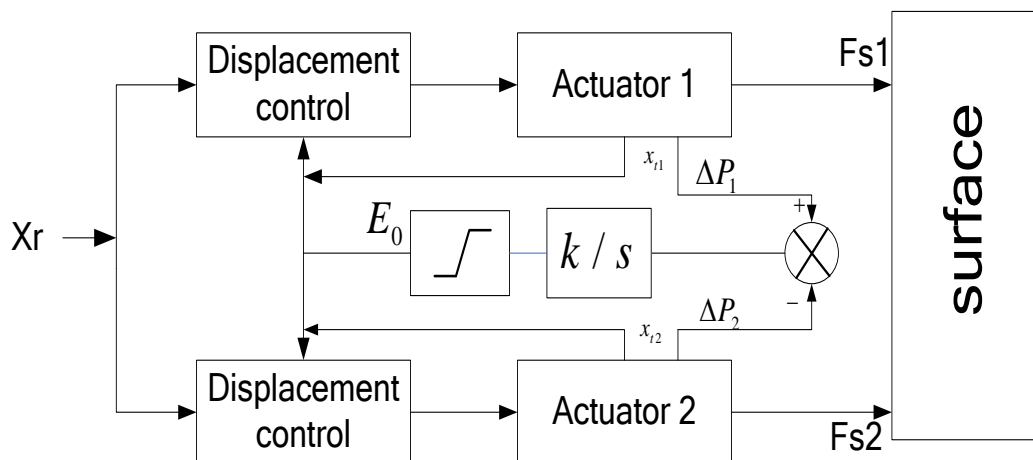


Figure 5. Control Diagram of Static Force-fight

The integral is used because the strategy is designed for static control while the integral only impact on low frequency part and has little impact on dynamic process, when there is difference between F_{s1} and F_{s2} , the integral of fighting-force is translated into displacement compensation signals E_{o1} and E_{o2} to adjust the control current of each channel until the force-fight is eliminated.

The simulation results is presented in figure 6 when the dead zone of servo-valve 1 and servo-valve 2 is 0.012mm and 0.024mm respectively and the system is no-load, a step current signal of 0.5V is applied.

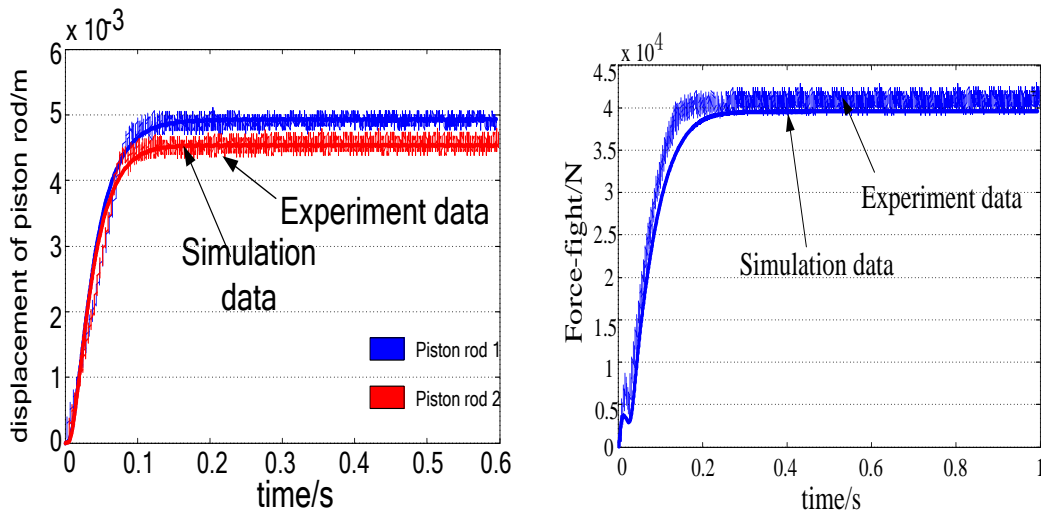


Figure 6. Test and Simulation without Control Strategy

As show in Figure 6 without control strategy the fighting-force reaches around 40KN and the difference of the two piston rods' displacement is around 0.4mm. In Figure 7 the control strategy is applied:

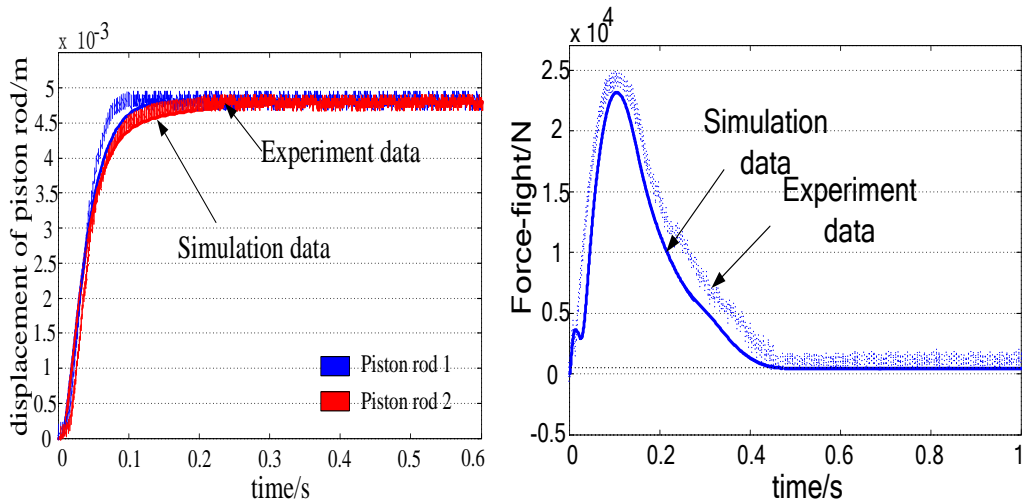


Figure 7. Test and Simulation with Control Strategy

As show in Figure 7 the static fighting-force is reduced to 500N which means the force-fight has been eliminated basically compared with 40KN and the strategy of force equilibrium is proved to be very effective.

5.2. Elimination of Dynamic Force-Fight

Although the force equilibrium can solve the problem of static force-fight well, the dynamic fighting-force is still great as show in Figure 7 which is around 25KN and it is big enough to lead to the fatigue of rudder surface and destroy the structure during longtime service. In order to improve the dynamic performance and reduce the dynamic fighting-force, adopting the PID controller to realize force equilibrium instead of simply using an integral link, the structure diagram is presented as:

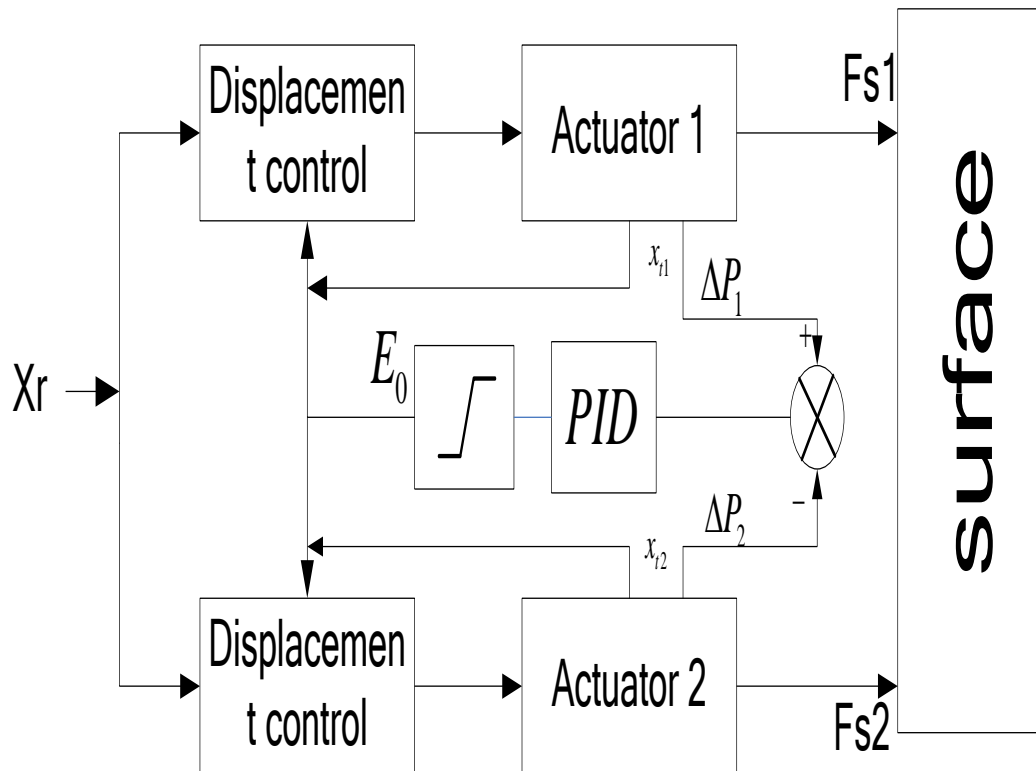


Figure 8. Control Strategy with PID Controller

The integral link controls the static fighting-force, differential link control the dynamic fighting-force and the proportion link speed the convergence of force equilibrium.

The steps of debugging PID parameters are expressed as:

First step: determine the proportion gain κ_p : Make the coefficient of integral and differential to be zero and the value of input signal is set to 60%~70% of the maximum. Increase the value of κ_p until oscillation appears. Then reduce κ_p from current value until oscillation disappears. The value at this point multiplied by 0.6~0.7 is the ultimate value of κ_p .

Second step: determine the integral time constant T_i : After proportion gain is determined, set a larger integral time constant firstly and then reduce the value until oscillation appears, then in turn increase this value until oscillation disappears, the value at this point multiplied by 1.5~1.8 is the final value of T_i .

Final step: determine the differential time constant T_d : The way of determining T_d is the same as κ_p , take 30% of the value when oscillation disappears as the final T_d .

The parameter of the PID controller designed in this system can be calculated using the method above, the values are $\kappa_p = 1 \times 10^{-7}$, $\kappa_i = \kappa_p / T_i = 1 \times 10^{-6}$, $\kappa_d = \kappa_p \cdot T_d = 2 \times 10^{-10}$.

The simulation and tests results of adapting the dynamic force-fight strategy is presented in figure 9 when the dead zone of servo-valve 1 and servo-valve 2 is 0.012mm and 0.024mm respectively and the system is no-load, a step current signal of 0.5V is applied.

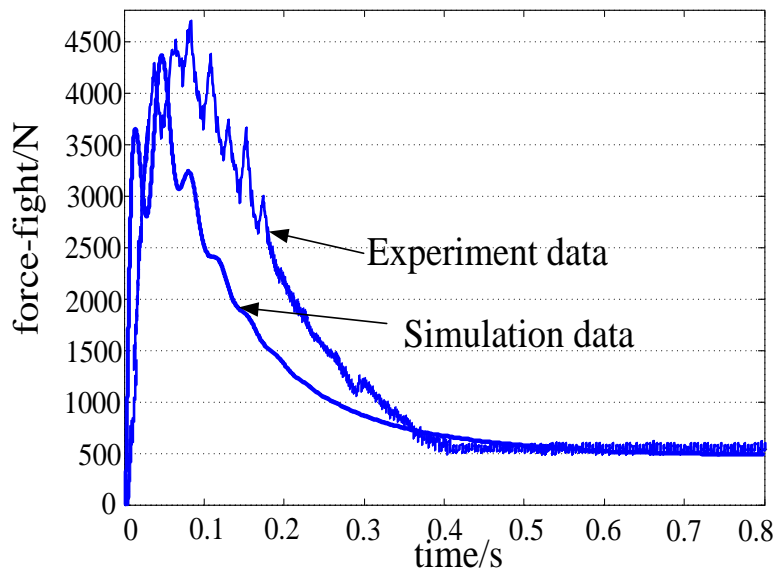


Figure 9. Test and Simulation with PID Controller

Test and simulation results show that, adapting the PID controller to compensate displacement signal the dynamic fighting-force reduce to around 4500N from 25KN and the static fighting-force maintains around 400N.

6. Conclusion

- (1)The mathematical model can simulate the real system accurately;
- (2)Adopting the integral of pressure differential of the two cavities as displacement compensation can basically eliminate static fighting-force;
- (3)PID controller can effectively reduce both the static and dynamic fighting-force.

Acknowledgements

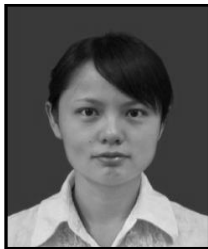
I would like to extend my sincere gratitude to my tutor, for his instructive advice and useful suggestions on my theses. Special thanks should go to my friends who have put considerable time and effort into their comments on the draft. This work was financially supported by National Natural Science Foundation of China under the Grant „study of nonlinear control allocation for tailless flying-wing aircraft under low speed “.No. 61374032/2013.

References

- [1] Z. Wang, L. Qiu and X. Zhang, *et al.* “Research on the synchronous drive of the redundant channels for hydraulic actuator [J]”, *Journal of Astronautics*, vol. 12, no. 2, (1991), pp. 9-14.
- [2] M. Wang, X. Ma, ”Research on the test-method of force-fight on redundant actuator system [J]”, *Civil Aircraft Design and Research*, vol. 2, (2010), pp. 12-15.
- [3] T. Cheng and Z. Wang, “Study of the parallel actuation of smart actuators [J]”, *Journal of Beijing University of Aeronautics and Astronautics*, vol. 22, no. 2, (1996), pp. 167-170.
- [4] H. Straub Henrik and C. Roland, “Boeing 747-400 upper rudder control system with triple tandem valve [C]”, *Aerospace Technology Conference and Exposition*, Long Beach, CA, United States, (1991), pp. 31-40.

- [5] A. F. Yahya, "Fundamental design concepts in multi-lane smart electromechanical actuators [J]", *Smart Materials and Structures*, (2005), vol. 14, no. 6, pp.1227-1238.
- [6] M. O'brien, "Boeing 777 thrust reverser actuation system", *Aircraft Engineering and Aerospace Technology*, (1998), vol. 70, no. 5, pp. 364-366.
- [7] C. Olar, H. Susan, Carl Udo B., "Concepts for position and load control for hybrid actuation in primary flight controls [J]. *Aerospace Science and Technology*, (2007), vol. 11, no. 2, pp. 194-201.
- [8] J.-C. Maré, "Comparison of Hydraulically and Electrically Powered Actuators with reference to Aerospace Applications[C]", *Hydraulics and Pneumatics Conference*, vol. 10, (2007).
- [9] S. Wang, M. Cui and J. Shi, *et al.* "Performance degradation reliability analysis for redundant actuation system [J]", *Chinese Journal of Aeronautics*, (2005), vol. 18, no. 4, pp. 359-365.
- [10] X. Song and W. Meng, "Study on aircraft aileron actuator control assembly ground testboard [M]", Xi'an: Northwestern Polytechnical University, vol. 3, (2011).
- [11] Z. Wang, S. Guo and W. Li, "Modeling, simulation and optimal control for an aircraft of aileron-less folding wing [J]", *WSEAS Transactions on Systems and Control*, vol. 3, no. 10, (2008), pp. 869-878.
- [12] K. C. Patra, "Engineering fluid mechanics and hydraulic machines [M]", Oxford U. K., Alpha Science International, (2011).
- [13] J. Tao, S. Wang and Z. Jiao, "Reliability analysis with performance for triple redundant actuator [J]", *Journal of System Simulation*, vol. 16, no. 1, (2004), pp. 38-41.
- [14] K. Nagai, Y. Dake and Y. Shiigi, *et al.* "Design of redundant drive joints with double actuation using springs in the second actuator to avoid excessive active torques [C]", 2010 IEEE International Conference on Robotics and Automation (ICRA), Anchorage, AK, (2010), pp. 805-812.
- [15] J. Zhang, F. Gao and H. Yu, *et al.* "Design and development of a novel redundant and fault-tolerant actuator unit for heavy-duty parallel manipulators [J]", *Journal of Mechanical Engineering Science*, vol. 225, no. 12, (2011), pp. 3031-3044.

Authors



Ying Zhang, She was born in Wuhan (China), on September 2, 1984. She received her M.Sc. in Mechanical Engineering from Northwestern Polytechnical University. Now she is reading a doctorate in Detection Technology and Automatic Equipment. Her current research interests include servo control and design of hydraulic system.



Zhaohui Yuan, He was born in Anhui (China), on March, 1964. He received M.Sc. in Transmission and control of fluid and PhD in Detection Technology and Automatic Equipment. Now he is full professor in School of automation, Northwestern Polytechnical University. His current research interests include different aspects of servo control Systems.